4

Interaction of electromagnetic radiation with the Earth's atmosphere

In chapter 3, we discussed principally the interaction of electromagnetic radiation with the surface and bulk of the material being sensed. However, the radiation also has to make at least one journey through at least part of the Earth's atmosphere, and two such journeys in the case of systems that detect reflected radiation, whether artificial or naturally occurring. Each time radiation passes through the atmosphere it is attenuated to some extent. In addition, as we have already seen in section 3.1.2 and figure 3.4, the atmosphere has a refractive index that differs from unity so that radiation travels through it at a speed different from the vacuum speed of 299 792 458 m s^{-1}. These phenomena must be considered if the results of a remotely sensed measurement are to be corrected for the effects of atmospheric propagation, or if they are to be used to infer the properties of the atmosphere itself. We have already considered them in general terms in discussing the radiative transfer equation (section 3.4). In this chapter, we will relate them more directly to the constituents of the atmosphere.

4.1 Composition and structure of the gaseous atmosphere

At sea level, the principal constituents of the dry atmosphere are molecules of nitrogen (about 78% by volume), oxygen (21%) and the inert gas argon (1%). There is also a significant but variable (typically 0.1% to 3%) amount of water vapour, often specified by the *relative humidity* H. This is defined by equation (4.1):

$$H = \frac{p_{\text{water}}}{p_{\text{sat}}(T)} \tag{4.1}$$

as a fraction between zero and 1 (or more commonly as a percentage), where p_{water} is the *partial pressure* of the water vapour, which can be defined as the product of the total atmospheric pressure with the volume fraction of water vapour, and $p_{\text{sat}}(T)$ is the saturated vapour pressure of water at temperature T. Figure 4.1 shows the variation of the saturated vapour pressure of water with temperature. As an example, at 20°C $p_{\text{sat}} = 2.34$ kPa, so if the total atmo-

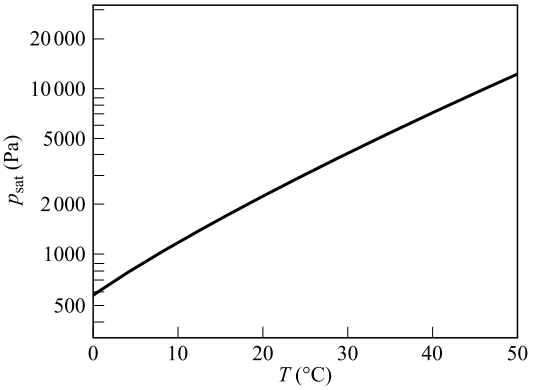

Figure 4.1. Temperature dependence of the saturated vapour pressure of water.

spheric pressure is 100 kPa and the relative humidity is 80%, the volume fraction of water vapour is 1.9%.

In addition to the gases already mentioned, the atmosphere contains a regionally variable quantity of carbon dioxide (currently about 0.035% by volume) and traces, measured in parts per million, of many other gases. Table 4.1 summarises the normal gaseous composition of the atmosphere.

Atmospheric pressure and density diminish with height above the Earth's surface. This is because the molecules, acted upon by gravity, tend to sink to

Table 4.1. Gaseous constituents of the Earth's atmosphere

The third column shows the fraction by volume of the gas at sea level, and the fourth column shows the total mass of gas found in a column through the entire atmosphere

Gas	Chemical formula	Volume fraction	Total mass kg m^{-2}
Nitrogen	N_2	0.7808	7797
Oxygen	O_2	0.2095	2389
Argon	Ar	9.34×10^{-3}	133
Carbon dioxide	CO_2	3.5×10^{-4}	5.6
Neon	Ne	1.8×10^{-5}	0.13
Helium	He	5.2×10^{-6}	7.5×10^{-3}
Methane	CH_4	1.8×10^{-6}	1.0×10^{-2}
Krypton	Kr	1.1×10^{-6}	3.4×10^{-2}
Carbon monoxide	CO	$0.06 - 1 \times 10^{-6}$	$0.06 - 1 \times 10^{-2}$
Sulphur dioxide	SO_2	1.0×10^{-6}	2.9×10^{-2}
Hydrogen	H_2	5.0×10^{-7}	4.0×10^{-4}
Ozone	O_3	$0.01 - 1 \times 10^{-6}$	5.4×10^{-3}
Nitrous oxide	N_2O	2.7×10^{-7}	4.0×10^{-3}
Xenon	Xe	9.0×10^{-8}	4.0×10^{-3}
Nitric oxide	NO_2	$0.05 - 2 \times 10^{-8}$	$0.02 - 4 \times 10^{-4}$
Total dry atmosphere		1	1.032×10^4
Water vapour	H_2O	0.001 – 0.028	6.5 – 180

the surface but are prevented from doing so fully by thermal excitation. The distribution of density with height is thus governed by the Boltzmann distribution and is approximately exponential. There are, however, significant variations from this approximate dependence and it is conventional to divide the atmosphere into several layers. The lowest of these is the *troposphere* (approximately 0–11 km above the Earth's surface), in which the temperature decreases with height; this is overlain by the *stratosphere* (11–50 km), in which the temperature is roughly constant up to about 35 km, then increases with height; the *mesosphere* (50–80 km); and the *thermosphere* (above about 80 km). The height ranges just specified are for typical conditions at temperate latitudes: there is considerable seasonal and latitudinal variation. Figure 4.2 shows the variation of temperature, pressure and density of the standard (mid-latitude) atmosphere with height.

The absolute temperature T, pressure p and density ρ of the atmosphere can be assumed to be related to one another by

$$\frac{\rho T}{p} = \frac{M_m}{R} \tag{4.2}$$

where M_m is the mass of one mole of atmospheric gas and R is the gas constant (8.314 J K^{-1}). This equation is based on the assumption that the atmosphere behaves as an ideal gas. For heights up to about 100 km, M_m has a more or less constant value of about 0.02896 kg.

The atmospheric pressure p at a height z is a measure of the mass of air, and hence the number of molecules, above z. This follows because the Earth's gravitational field strength g may be assumed to be constant over the range of heights for which p is significant, so that

$$p(z) = M_m g \int_z^\infty N(z')\, dz' \tag{4.3}$$

where $N(z')$ is the molar concentration (number of moles per unit volume) at height z'. For example, figure 4.2b shows that the pressure falls to half its sea-level value at about 5.5 km, and to 1% at about 31 km, so we may state that half of the atmosphere, by mass, is found below 5.5 km and 99% below 31 km. A spaceborne remote sensing system thus looks through all of the atmosphere, while an airborne system typically looks through only a quarter of it. The variation of pressure with height can be modelled rather crudely as an exponential,

$$p(z) = p_0 \exp\left(-\frac{z}{z_0}\right) \tag{4.4}$$

equivalent to assuming that the graph of figure 4.2b is a straight line, which will be convenient for considering the behaviour of atmospheric sounding systems. For the troposphere, a value of z_0 (the *scale height*) of roughly 7.5 km is appropriate.

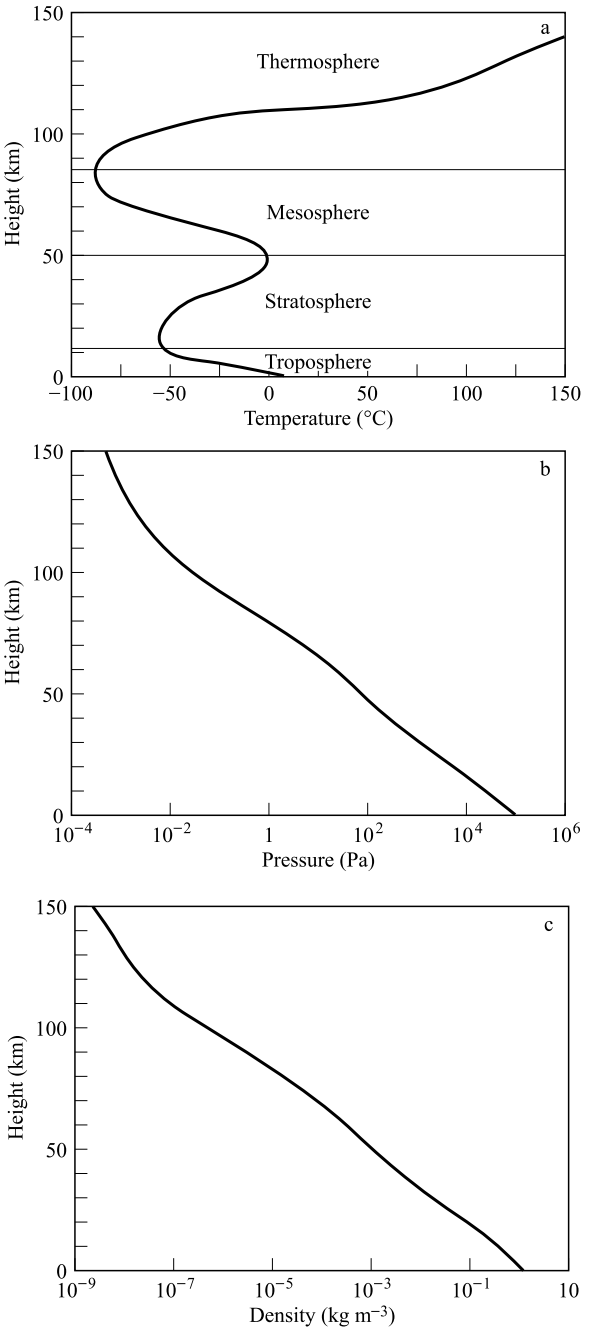

Figure 4.2. Variation with height of (a) temperature, (b) pressure and (c) density of the standard atmosphere.

Graphs similar to figure 4.2b can also be drawn for the partial pressures of the individual molecular species listed in table 4.1 that compose the atmosphere. Provided that we do not consider altitudes much above 100 km, where the heavier molecules are less favoured, and provided that the gas is 'well mixed', the graph will follow the shape of figure 4.2b fairly accurately. Most of the atmospheric gases are well mixed in this sense, with the notable exception of ozone, which, as well as being found in the troposphere, is also generated (by the action of solar ultraviolet radiation) in the stratosphere.

4.2 Molecular absorption and scattering

A detailed understanding of the processes by which molecules absorb and scatter electromagnetic radiation requires considerable knowledge of quantum mechanics, which is beyond the scope of this book.[1] We may state, however, that the energy of an individual molecule cannot be varied continuously, but must be one of a number, in principle infinite, of discrete values called *energy levels*. If a molecule absorbs electromagnetic radiation, it must be promoted from one energy level to another, and hence only certain values of the energy increase ΔE are allowed. Planck's law states that the frequency f of the electromagnetic radiation is given by

$$\Delta E = hf \tag{4.5.1}$$

where h is Planck's constant, although it is often more convenient to write this equation in terms of the angular frequency ω:

$$\Delta E = \frac{h}{2\pi}\omega = \hbar\omega \tag{4.5.2}$$

Thus, we expect that molecules will absorb 'selectively', at particular frequencies, which are usually called *absorption lines*.

4.2.1 Mechanisms of molecular absorption

There are three main mechanisms by which molecules can absorb electromagnetic radiation. The first of these, requiring the largest amounts of energy, involves the promotion of electrons to higher energy levels. These are termed *electronic transitions*. Calculation of the energy levels for any but the simplest of molecules is an extremely difficult task, so we will illustrate the idea with reference to the hydrogen atom. In this case, the electronic energy levels are given by

$$E_n = -\frac{me^4}{32\pi^2\varepsilon_0^2\hbar^2}\frac{1}{n^2}$$

[1] Schanda (1986) gives a considerably more detailed account.

where m is the electron mass (strictly, the electron's reduced mass, which, in the hydrogen atom, is 99.95% of the electron mass) and n is a *quantum number* that can take only positive integer values. Substituting the values of the constants into the formula, we find that

$$E_n = -\frac{2.177 \times 10^{-18}\text{J}}{n^2}$$

although it is often more convenient to use the *electron-volt* (symbol eV) as the unit of energy, where $1\,\text{eV} \approx 1.602 \times 10^{-19}\text{J}$, so that the formula becomes

$$E_n = -\frac{13.59\,\text{eV}}{n^2}$$

In its *ground state* (the configuration with lowest energy), hydrogen has $n = 1$. The smallest increase in energy therefore corresponds to the transition from $n = 1$ to $n = 2$, which requires an increase in energy of 10.2 eV. This is typical of the energies required for electronic transitions, and from equation (4.5.1) we see that the frequency of the electromagnetic radiation needed to cause such transitions will therefore be of the order of 10^{15} Hz.[2] The corresponding wavelength is thus a few tenths of a micrometre, so that we expect to find the absorption lines due to electronic transitions in the ultraviolet and visible regions of the electromagnetic spectrum.

The second mechanism of molecular absorption that we shall consider is vibration. The molecular bond between atoms behaves more or less like a spring. To model this, we will consider a diatomic molecule consisting of two atoms, with masses m_1 and m_2, connected by a spring with force constant (defined as $dF/d\text{x}$, where F is the tension and x is the extension) k, as shown in figure 4.3. Classical physics gives the natural angular frequency of this system as

$$\omega_0 = \sqrt{\frac{k(m_1 + m_2)}{m_1 m_2}} \tag{4.6}$$

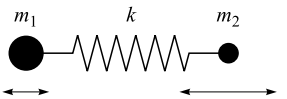

Figure 4.3. Classical model of molecular vibration. Atoms of masses m_1 and m_2 are connected by a spring of force constant k.

[2] Note that in molecular spectroscopy, it is common to specify the frequency of a transition using its *wavenumber*, normally defined as $1/\lambda$, where λ is the wavelength. For example, the wavenumber of the $n = 1 \rightarrow 2$ transition for atomic hydrogen is about $82\,000\,\text{cm}^{-1}$. Note that the spectroscopist's definition of wavenumber differs from the physicist's definition (equation (2.6)) by a factor of 2π.

and quantum mechanics gives the energy levels as

$$E_v = \left(v + \frac{1}{2}\right)\hbar\omega_0 \tag{4.7}$$

where v is a quantum number that can take any non-negative integer value. This quantum number can change only by ± 1, so in fact the only possible amount of energy that can be absorbed is $\Delta E = \hbar\omega_0$, giving an absorption line at the resonant frequency $f = \omega_0/2\pi$. Because the force constant k is of the order of 1000 N m^{-1}, the resonant frequency is typically between 10^{13} and 10^{14} Hz, corresponding to wavelengths generally in the thermal infrared region.

The last absorption mechanism we shall discuss is rotation. We will consider a simple diatomic molecule consisting of two atoms, with masses m_1 and m_2, separated by a fixed distance d (figure 4.4). Classically, this system can rotate about the centre of mass of the two atoms. The moment of inertia of the system is given by

$$I = \frac{m_1 m_2}{m_1 + m_2} d^2 \tag{4.8}$$

and, according to quantum mechanics, the energy of such a state is given by

$$E_J = \frac{J(J+1)\hbar^2}{2I} \tag{4.9}$$

where J is a quantum number that can take any non-negative integer value. When electromagnetic radiation is absorbed, J must increase by 1. Calculating ΔE from equation (4.9), for the transition from quantum number J to $J+1$, and substituting into equation (4.5), we find that the frequency of a rotation absorption line is given by

$$f = \frac{(J+1)h}{4\pi^2 I}$$

As an example, we can consider the carbon monoxide molecule. This has $m_1 = 2.66 \times 10^{-26}$ kg, $m_2 = 1.99 \times 10^{-26}$ kg and $d = 1.13 \times 10^{-10}$ m, giving it a moment of inertia $I = 1.45 \times 10^{-46}$ kg m^2. We thus calculate that the $J = 0 \rightarrow 1$ transition will occur at a frequency of 116 GHz, which is in the microwave region. In general, we expect to find the rotational absorption lines in the microwave or far-infrared regions of the electromagnetic spectrum, with frequencies typically between 10^{10} and 10^{12} Hz.

Although we have now outlined the most important mechanisms governing molecular absorption lines, there are further complications to be considered. *Combinations* of mechanisms can operate at the same time. For example, the

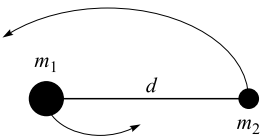

Figure 4.4. Classical model of molecular rotation. Atoms of masses m_1 and m_2, separated by distance d, rotate about their common centre of mass.

energy level of a molecule can be described by both a rotational quantum number J and a vibrational quantum number v, and both of these may change in a transition. This gives rise to a more complicated vibrational–rotational spectrum in which a vibrational absorption line has fine structure superimposed on it as a result of different rotational transitions. We should also note that not all possible transitions can in fact be excited by electromagnetic radiation. For example, the hydrogen molecule H_2 has a symmetric distribution of electric charge,which means that, classically speaking, an electric field cannot exert a force on it. We should therefore not expect molecular hydrogen to absorb electromagnetic radiation by vibrational or rotational transitions.

We have implicitly suggested that a molecular transition occurs at a single frequency, so that the absorption line in the spectrum has a width of zero. In fact, all lines are broadened to some extent. The Heisenberg uncertainty principle imposes a minimum line width, although this is negligible compared with other sources of line-broadening. In proportion to the frequency of the line, the effect is largest for electronic transitions, and even for these it is only of the order of 1 part in 10^8. Much more significant is the effect of thermal motion of the gas. The line width Δf due to this effect, which is usually called *Doppler broadening*, is given by

$$\frac{\Delta f}{f} = \sqrt{\frac{RT}{M_m c^2}} \tag{4.10}$$

where f is the frequency of the line, R is the gas constant, T is the absolute temperature, M_m is the mass of one mole of the gas, and c is the speed of light. Equation (4.10) shows that increasing the temperature will broaden the line, and that heavier molecules will exhibit narrower lines than lighter molecules. The fractional broadening due to this effect is typically 1 part in 10^6.

Another important mechanism is *pressure broadening*, also called *collision broadening*. The molecules of the gas collide with one another and with other molecules in the atmosphere, and these collisions disturb the state of the molecule. The pressure broadening can be written approximately as

$$\Delta f \approx \frac{\sigma N_A p}{\sqrt{M_m RT}} \tag{4.11}$$

where p is the gas pressure, σ is related to the collision cross-section for the molecules, and is of the order of 10^{-19} m^2, and N_A is the Avogadro number.

We can illustrate these formulae with two examples. First, we consider the 0.76 μm absorption line of O_2 at an altitude of 50 km, near the top of the stratosphere. The temperature at this altitude can be taken as 271 K, so equation (4.10) gives the Doppler broadening $\Delta f/f$ as 9×10^{-7}. The pressure is about 80 Pa, so equation (4.11) gives the pressure broadening as $\Delta f \approx 6 \times 10^5$ Hz, and hence $\Delta f/f \approx 1.5 \times 10^{-9}$. In this case Doppler broadening dominates, and the line width can be specified as 3.5×10^8 Hz or about 0.01 cm^{-1}. Our second example is the 22.2 GHz absorption line of H_2O at sea level. Taking the temperature as 288 K, we find from equation (4.10) that the Doppler broad-

ening is $\Delta f/f = 1.2 \times 10^{-6}$, and taking the pressure as 10^5 Pa, equation (4.11) gives the pressure broadening as $\Delta f/f = 4.1 \times 10^2$. In this case the pressure broadening dominates, and the line width is approximately 0.9 GHz (0.03 cm^{-1}).

Table 4.2 summarises the main absorption lines in the Earth's atmosphere.

4.2.2 Molecular scattering

If we model a molecule very simply as an electrically conducting sphere of radius a, much smaller than the wavelength λ of the radiation, it will have a polarisability

$$\alpha = 4\pi\varepsilon_0 a^3$$

(this follows from equation (3.76) by setting the refractive index $n = \infty$), and hence a scattering cross-section, given by equation (3.77), of

$$\sigma_s = \frac{128\pi^5 a^6}{3\lambda^4} \tag{4.12}$$

Table 4.2. Principal molecular absorption lines in the Earth's atmosphere

Visible–infrared region			
Wavelength (μm)	**Molecule**	**Wavelength (μm)**	**Molecule**
0.26	O_3	3.9	N_2O
0.60	O_3	4.3	CO_2
0.69	O_2	4.5	N_2O
0.72	H_2O	4.8	O_3
0.76	O_2	4.9	CO_2
0.82	H_2O	6.0	H_2O
0.93	H_2O	6.6	H_2O
1.12	H_2O	7.7	N_2O
1.25	O_2	7.7	CH_4
1.37	H_2O	9.4	CO_2
1.85	H_2O	9.6	O_3
1.95	CO_2	10.4	CO_2
2.0	CO_2	13.7	O_3
2.1	CO_2	14.3	O_3
2.6	H_2O	15	CO_2
2.7	CO_2		
Microwave region			
Frequency (GHz)	**Molecule**	**Frequency (GHz)**	**Molecule**
22.2	H_2O	119	O_2
60	O_2	183	H_2O

This rather crude model describes Rayleigh scattering by individual molecules. We can estimate the region of the electromagnetic spectrum in which it is important as follows.

From equation (4.3) we know that the molar concentration (number of moles per unit volume) of the molecules in the atmosphere, integrated through the whole atmosphere, is given by

$$\frac{p_0}{M_m g}$$

where p_0 is the sea-level pressure, M_m the molar mass of the molecules and g the gravitational field strength. Thus, we can estimate the optical thickness of the atmosphere due to molecular Rayleigh scattering as

$$\tau_s \approx \frac{N_A p_0}{M_m g} \frac{128\pi^5 a^6}{3\lambda^4}$$

where N_A is Avogadro's number. Assuming that this scattering is significant when $\tau_s > 1$, and substituting the values $p_0 = 10^5$ Pa, $M_m = 0.029$ kg, $a = 10^{-10}$ m, $N_A = 6 \times 10^{23}$, $g = 10$ m s^{-2}, we find that λ must be less than about 0.25 μm. Thus, molecular Rayleigh scattering is significant mainly in the ultraviolet region of the electromagnetic spectrum, although it is also noticeable in the visible region. The λ^{-4} dependence of equation (4.12) implies that blue light will be very much more strongly scattered than red light, and this is the reason why the clear sky appears blue, since visible skylight is mainly due to molecular scattering. It is also the principal explanation of red skies in the region of the rising and setting sun, since here the sunlight has travelled through a very long atmospheric path so that significant amounts of blue light have been scattered away from the forward direction. The strong atmospheric scattering of blue light, and especially of ultraviolet radiation, is the reason that these wavelengths are normally less important in remote sensing than are the longer wavelengths.

Other molecular scattering mechanisms also occur. In particular, scattering cross-sections are very much larger than implied by equation (4.12) at frequencies close to absorption lines. This phenomenon is known as *resonant absorption*. Molecular fluorescence effects can also cause large scattering cross-sections.

Figure 4.5 attempts to summarise the practical implications of sections 4.2.1 and 4.2.2, by illustrating the optical thickness due to the attenuation (i.e. scattering and absorption) of electromagnetic radiation propagating vertically through the entire atmosphere. The figure is rather schematic, since it does not resolve fine spectral details and assumes 'standard' atmospheric conditions. (An alternative presentation of the information in figure 4.5 is given in figure 1.1.) The comparative transparency of the optical region and of the microwave region below the 60 GHz oxygen absorption line is clearly apparent, as is the complexity of the infrared region as a result of the large number of molecular transitions. The comparatively transparent regions define the so-called *atmo-*

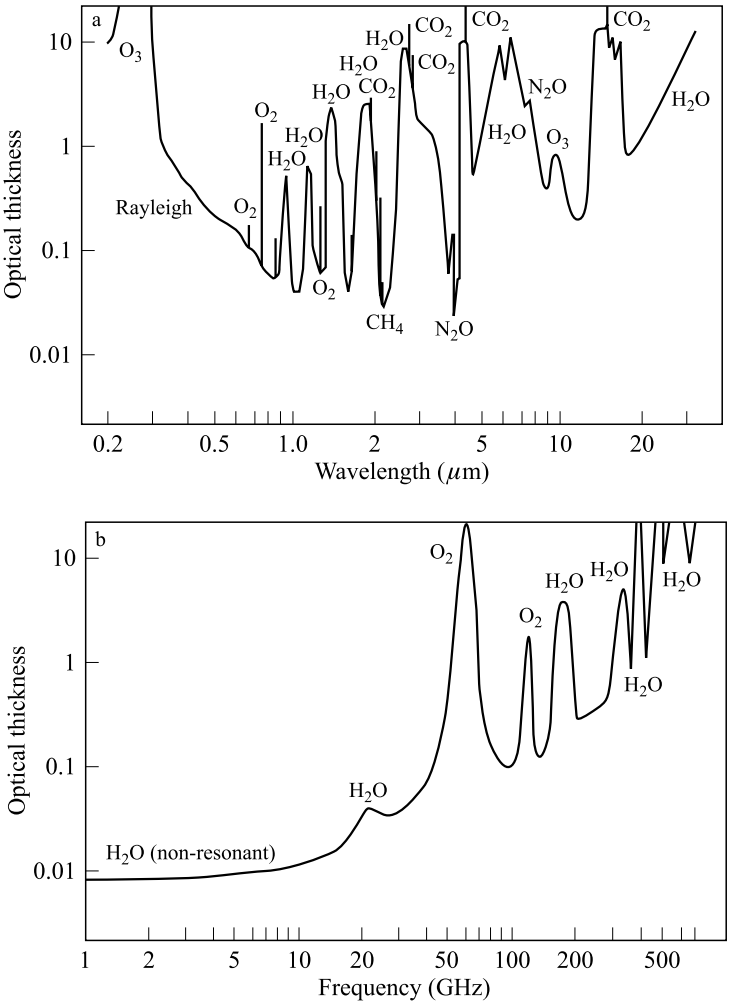

Figure 4.5. Total zenith optical thickness of the standard atmosphere: (a) ultraviolet, optical and infrared region; (b) microwave region.

spheric windows. Roughly speaking, there are two main windows: one in the optical-infrared region and the other in the microwave region. These can, however, be usefully subdivided by the presence of absorption lines.

Figure 4.5 shows the optical thickness of the atmosphere for a vertically propagating ray. If the ray travels obliquely through the atmosphere, however, it is clear that it will encounter a larger number of molecules, so we would expect the optical thickness to be increased. We can derive a very simple model of this phenomenon by assuming that the Earth is flat, and considering a ray that makes an angle θ to the horizontal. The optical thickness is given by

$$\tau = \int_0^\infty \gamma(x)\, dx$$

where $\gamma(x)$ is the attenuation coefficient at distance x along the ray. We know that x is related to the height z in the atmosphere by

$$x = \frac{z}{\sin\ \theta}$$

so we can rewrite our expression for the optical thickness as

$$\tau = \frac{1}{\sin\ \theta} \int_0^\infty \gamma(z)\ dz$$

In other words, the optical thickness is increased by a factor of $1/\sin(\theta)$ with respect to its value for a vertical ray. This very simple formula is sufficiently accurate for θ greater than about 15°; that is, for factors up to about 4. For smaller angles, it is necessary to take the Earth's curvature into account. (This is obvious, because the $1/\sin(\theta)$ formula implies that the optical thickness is infinite for a horizontal ray, whereas we know that such a ray will, because of the Earth's curvature, emerge from the atmosphere and hence propagate within it for a finite, and not infinite, distance.) The required correction depends on the distribution of the attenuation coefficient with height, which we can model as an exponential decay

$$\gamma(z) = \gamma(0)\ \exp\left(-\frac{z}{z_0}\right)$$

where z_0 is the scale height. Note that this is analogous to the simple model of the distribution of atmospheric pressure with height that we introduced in equation (4.4), and we expect that for most atmospheric species the appropriate value of z_0 will be about 8 km.

Figure 4.6 shows the factor by which the optical thickness for oblique propagation is increased relative to vertical propagation, for three values of the scale height z_0. Figure 4.6a shows the range of θ from 0 to 15°, and it can be seen that the effect of the scale height is significant in this range. Figure 4.6b shows the range from 15° to 90°. Here, the simple $1/\sin(\theta)$ formula is accurate, so only one curve is shown.

4.3 Microscopic particles in the atmosphere: aerosols

In the preceding sections we have considered the gaseous composition of the atmosphere. However, it also contains solid and liquid components that can have a significant effect on the propagation of electromagnetic radiation. These components generally exhibit much greater spatial and temporal variability than the gaseous components, so they are rather harder to characterise. In this section we discuss aerosols, and in the following section the larger ice and water particles that constitute fog, cloud, rain and snow.

Aerosols (atmospheric *haze*) are suspensions of very small solid particles or liquid droplets, with radii typically in the range 10 nm to 10 μm. They can be regarded as being suspended in the atmosphere since, because of their small

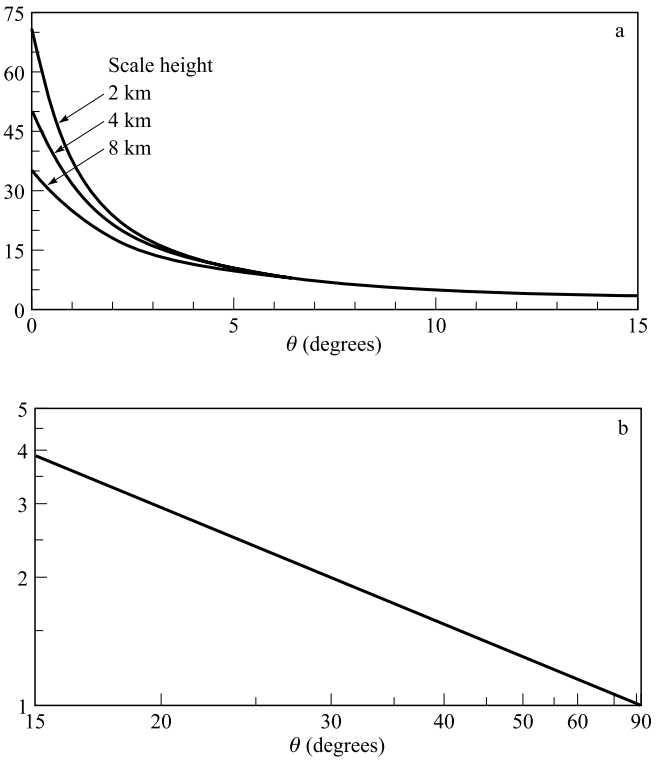

Figure 4.6. The factor by which the optical thickness of the atmosphere is increased for oblique propagation relative to vertical propagation. θ is the angle to the horizontal. (a) The range 0–15°, showing the effect of the scale height of the attenuating medium; (b) the range 15–90°, in which the influence of the scale height is negligible. Figuure 4.6b has been plotted with logarithmic scales to emphasise the $1/\sin(\theta)$ dependence.

size, the speed at which they fall under gravity is very small. For example, a particle of radius 1 μm will fall at something like 10^{-4} m s^{-1}, which means that under conditions of absolutely still air it would take of the order of 100 days to fall through 1 km.

Most aerosols are found in the atmospheric *boundary layer*, the lowest kilometre or so of the atmosphere in which transport processes are dominated by wind turbulence and by atmospheric convection.[3] This indicates that the aerosols are largely generated from the Earth's surface, for example in liberating and then carrying aloft solid microscopic dust particles from the land surface and water droplets from the ocean surface. Consequently, the type and size distributions of aerosols are strongly dependent on the local meteorological conditions and the local nature of the Earth's surface – whether urban, rural, oceanic, volcanic, and so on. For visible-wavelength radiation (say a wavelength of 0.55 μm), the attenuation coefficient at sea level typically ranges

[3] Aerosols are, however, also found in the stratosphere.

between 0.05 and 0.5 km^{-1}, and the total (vertical) optical thickness of a tropospheric aerosol is typically 0.1 to 1. If we compare this range of values with the gaseous optical thickness at wavelength 0.55 μm of about 0.2, as shown in figure 4.5a, we can see that the aerosol component of the atmosphere is radiatively significant.

The attenuation coefficient of an aerosol at optical and infrared wavelengths is dominated by scattering rather than absorption. The dependence of the attenuation coefficient on wavelength is usually represented approximately by the *Ångström relation*

$$\gamma = \gamma_0 \lambda^{-n} \tag{4.13}$$

where γ_0 is a constant and n is called the *Ångström exponent*. For particles that are very small compared with the wavelength, the Rayleigh scattering formula implies that $n = 4$, and for very large particles, the fact that the scattering cross-section is of the order of the geometrical cross-section implies that $n = 0$. For aerosols, the Ångström exponent n is usually between 0.2 and 2. Maritime aerosols usually exhibit the largest particle sizes (the modal droplet radius is around 0.2 μm) and the smallest values of n. For most other aerosols, the value of n is around 1, although at high altitudes (stratospheric and higher-altitude tropospheric aerosols) the very small particle sizes give $n \approx 2$.

4.4 Larger particles: fog, cloud, rain and snow

At any one time, about half of the Earth's surface will be covered by cloud. Visible-wavelength sensors, and to some extent those operating in other regions of the electromagnetic spectrum, will be limited by the presence of significant amounts of cloud cover, and this can be a serious problem in the case of spaceborne sensors that revisit a particular location comparatively infrequently (see chapter 10). For example, it has been estimated that a Landsat satellite, which revisits a particular location once every 16 days, will obtain a cloud-free scene of a particular location in Britain only once per year, and a scene with 1 okta of cloud (an okta is one eighth of the sky obscured by cloud) only twice per year. The probability of less than 10% cloud cover in a single Landsat observation over the continental USA is about 0.05 to 0.4, and the number of observations needed to obtain a probability of 75% of less than 10% cloud cover is between 5 and 100 (Goetz, 1979). In high-latitude regions, the problems of cloud cover can be significantly worse (Marshall et al., 1994).

Precipitation can also have a significant effect on the propagation of electromagnetic radiation. In the case of rainfall, the rain rate is the dominant factor since this largely controls both the size distribution of the droplets and their number density.

The attenuation of electromagnetic radiation by these meteorological phenomena can be considered in both a positive and a negative light. For observations intended to characterise the Earth's surface, it is an inconvenience since it must be corrected for, or may even render the observation impossible. On the

other hand, it may be possible to derive useful information about the meteorological phenomenon itself from the effect on radiation, for example in microwave rain radars.

Fog and low-altitude (up to about 3000 m) cloud consists of water droplets, but these are very much larger than the droplets in aerosols, having modal radii from 10 to 50 μm. At visible and infrared wavelengths, scattering is again dominant. We can model the scattering fairly crudely by assuming that all the droplets have the same radius a and that their scattering cross-section is just the geometrical area πa^2. If the number density of the droplets (the number of droplets per unit volume) is N, the scattering coefficient is therefore given by

$$\gamma_s \approx \pi a^2 N$$

The mass density of liquid water in the fog or cloud is given by

$$\rho = \frac{4}{3}\pi a^3 N \rho_w \tag{4.14}$$

where ρ_w is the density of water, and we have assumed that the droplets are spherical, so we see that we can write the scattering coefficient as

$$\gamma_s \approx \frac{3\rho}{4a\rho_w} \tag{4.15}$$

Since the droplet radius is not strongly dependent on the mass density ρ, this equation implies that the scattering coefficient is roughly proportional to the mass density of liquid water in the cloud. This ranges from about 10^{-4} kg m^{-3} for fog and thin cloud, to about 10^{-2} kg m^{-3} for the densest clouds, so we should expect scattering coefficients in the region of 1 to 100 km^{-1}. Cloud layers are typically of the order of 1 km thick, so all but the thinnest clouds (and fog layers, which are typically 50 m thick) are optically opaque, with optical thicknesses in the range 1–100.

Similar remarks apply to the higher-altitude clouds that are composed of ice crystals. The crystals are of a similar size and density to the water droplets, and the calculation on which equation (4.14) is based is too crude to incorporate the fact that the ice crystals are not spherical.

We saw in section 3.4.2 that absorption dominates hugely over scattering for cloud droplets at microwave frequencies. Putting together equations (3.75) and (3.76), we see that the absorption cross-section of a small sphere of radius a and dielectric constant $\varepsilon' - i\varepsilon''$ is given by

$$\sigma_a = \frac{12\pi a^3 k \varepsilon''}{(\varepsilon' + 2)^2 + \varepsilon''^2}$$

where k is the wavenumber of the radiation. The dielectric constant of water in the microwave region can be described quite accurately using the Debye equation (3.20), and if we substitute this equation into our expression for σ_a we obtain

$$\sigma_a = \frac{12\pi a^3 k(1+\omega^2\tau^2)\omega\tau\varepsilon_p}{((\varepsilon_\infty+2)(1+\omega^2\tau^2)+\varepsilon_p)^2+\omega^2\tau^2\varepsilon_p^2}$$

for the absorption cross-section at angular frequency ω. Making the substitutions $\omega = ck = 2\pi f$ where f is the frequency, and approximating to the low-frequency limit $\omega\tau \ll 1$, we find

$$\sigma_a \approx \frac{48\pi^3\tau\epsilon_p}{(\varepsilon_\infty+\varepsilon_p+2)^2 c} a^3 f^2 \tag{4.16}$$

Although this expression appears complicated, the right-hand side is just a constant multiplied by a^3f^2. Multiplying this by the number density N of the water droplets to obtain the absorption coefficient, and making use of equation (4.14), we see that this simplified (low-frequency) model predicts that the absorption coefficient should be proportional to ρf^2, where ρ is the mass density of liquid water in the cloud. In fact, a somewhat more accurate approximation over the usual range of microwave frequencies is

$$\gamma_a \approx 0.6\left(\frac{\rho}{\mathrm{kg\,m^{-3}}}\right)\left(\frac{f}{\mathrm{GHz}}\right)^{1.9} \mathrm{dB\,km^{-1}} \tag{4.17}$$

Thus, we see that even a thick layer of dense cloud is comparatively transparent to microwave radiation, introducing of the order of 1 dB attenuation at 50 GHz. At frequencies below about 15 GHz, absorption by cloud is clearly negligible.

The water droplets in rain are roughly 100 times larger than those in clouds, being of the order of 1 mm in radius. At visible and infrared wavelengths, scattering is again dominant over absorption, and since the particle size is very much larger than the wavelength, the scattering cross-section of a droplet is of the order of the geometric cross-section. The angular distribution of the scattered radiation is, however, quite complicated – this fact is obvious from the existence of various rainbow phenomena.

The radii of the droplets in a particular rain shower are distributed over a rather large range. We can define a droplet size distribution $N(a)$, such that $N(a)\,da$ is the number of droplets per unit volume having radii between a and $a + da$, and various empirical forms of this distribution have been defined (e.g. Laws and Parsons, 1943; Marshall and Palmer, 1948; Joss and Gori, 1978). Assuming that the scattering cross-section of an individual drop is given by πa^2, the scattering coefficient is then

$$\gamma_s = \int_0^\infty \pi a^2 N(a)\, da \tag{4.18}$$

and the mass density of liquid water in the rain is

$$\rho = \int_0^\infty \frac{4}{3}\pi a^3 \rho_w N(a)\, da \tag{4.19}$$

where ρ_w is the density of water. The drop size distribution is mainly governed by the *rain rate*, usually specified in millimetres per hour. Table 4.3 illustrates the values calculated from equations (4.18) and (4.19) for rain rates of 1 mm h^{-1} (a light rainfall) and 100 mm h^{-1} (a tropical downpour), using the drop size distribution given by Joss and Gori (1978). If we assume that the scattering coefficient is proportional to the rain rate R raised to some constant power, the data of table 4.3 can be interpolated by equation (4.20):

$$\gamma_s = 4.9 \times 10^{-5} \left(\frac{R}{\text{mm h}^{-1}} \right)^{0.73} m^{-1} \tag{4.20}$$

Thus, we might expect the scattering coefficient in a heavy rain shower ($R = 25$ mm h^{-1}) to be of the order of 5×10^{-4} m^{-1} (about 2 dB km^{-1}).

The interactions between microwave radiation and rain are not so easy to calculate, because the droplets are similar in size to the wavelength of the radiation. The dimensionless parameter $x = 2\pi a/\lambda$ that determines whether the Rayleigh or Mie scattering formulae should be used can vary over a wide range as a result of the rather broad distribution of droplet sizes. Figure 4.7 shows the approximate dependence of the scattering and absorption coefficients on frequency for rain rates of 1 mm h^{-1} and 100 mm h^{-1}, from which it can be seen that (a) both scattering and absorption increase with rain rate, (b) absorption dominates over scattering except at high frequencies and rain rates, and (c) both absorption and scattering can be significant at frequencies above about 10 GHz.

4.5 The ionosphere

The ionosphere is an ionised layer above the Earth's atmosphere, extending from about 70 km to a few hundred kilometres above the surface. The ionisation is produced by extreme ultraviolet and X-radiation from the Sun, and it can have a significant effect on the propagation of radio-frequency electromagnetic radiation.

We saw in chapter 3 that the dielectric constant of a plasma is given by

Table 4.3. Calculated scattering coefficient and mass density of liquid water for two different rain rates

Rain rate (mm h^{-1})	γ_s (m^{-1})	ρ (kg m^{-3})
1	4.9×10^{-5}	3.3×10^{-5}
100	1.4×10^{-3}	2.2×10^{-3}

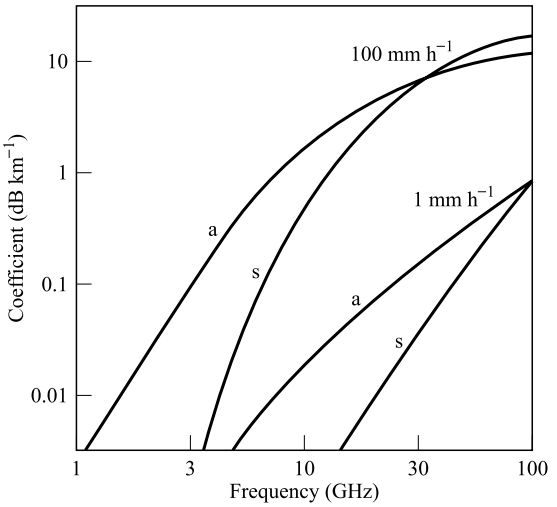

Figure 4.7. Typical microwave absorption (*a*) and scattering (*s*) coefficients for rainfall.

$$\varepsilon_r = 1 - \frac{Ne^2}{\varepsilon_0 m_e \omega^2} \tag{3.24}$$

where N is the number density of the electrons, e is the charge and m_e the mass of an electron, and ω is the angular frequency of the radiation. The plasma frequency is

$$\omega_p = \sqrt{\frac{Ne^2}{\varepsilon_0 m_e}} \tag{3.25}$$

and the dielectric constant is positive or negative according as ω is greater or less than ω_p. The maximum value of the electron density N in the ionosphere is of the order of $10^{12}\,\mathrm{m}^{-3}$, implying that ω_p is about $6 \times 10^7 \mathrm{s}^{-1}$ ($f_p \approx 9\,\mathrm{MHz}$). Thus, at microwave frequencies (and above) the dielectric constant is positive and very slightly less than 1.

We can use the binomial expansion to approximate the square root of equation (3.24) and hence obtain the refractive index of a plasma for the case when $\omega \gg \omega_p$:

$$n = \sqrt{\varepsilon_r} \approx 1 - \frac{Ne^2}{2\varepsilon_0 m_e \omega^2} \tag{4.21}$$

This is purely real, so there is no absorption of radiation. The phase velocity v of electromagnetic waves is given by equations (3.5) and (3.6) as

$$v = \frac{c}{n}$$

where c is the speed of light *in vacuo*, and in this case it is clearly greater than c. This seems paradoxical, since it appears to contradict Einstein's postulate that the speed of light represents an upper speed limit, until we recall that this speed

limit applies to the propagation of *information* and that, as discussed in section 3.1.3, the information in a wave is propagated at the group velocity and not the phase velocity.

Combining equations (3.5), (3.6) and (4.21), we may write the dispersion relation for radiation propagating in a plasma at a frequency very much higher than the plasma frequency as

$$\omega = \frac{ck}{1 - \dfrac{Ne}{2\varepsilon_0 m_e \omega^2}}$$

so we can evaluate the group velocity from equation (3.27):

$$v_g = \frac{d\omega}{dk} = \frac{c}{1 + \dfrac{Ne^2}{2\varepsilon_0 m_e \omega^2}} \tag{4.22}$$

This is clearly *less* than c, as expected. Furthermore, we can use equation (4.22) to calculate the time t taken for a pulse of radiation to travel through a finite region (for example, all) of the ionosphere. Since

$$t = \int \frac{dz}{v_g}$$

where z measures propagation distance, we obtain

$$t = \frac{z}{c} + \frac{e^2}{2\varepsilon_0 m_e \omega^2 c} \int N\, dz \tag{4.23}$$

The right-hand side of this expression can be interpreted as follows: the first term is just the time taken for light to travel the distance z *in vacuo*, and the second consists of a frequency-dependent constant multiplied by the integrated number-density of electrons along the path through the ionosphere.

As an example of the use of equation (4.23), consider the propagation of a pulse of microwaves at a frequency of 10 GHz vertically through the entire ionosphere. The value of $\int N\, dz$ in this case is typically 3×10^{17} m^{-2}, so the second term on the right-hand side of equation (4.23) has a value of 4.0×10^{-10} s. Thus, the pulse is delayed by 0.40 ns, or 0.12 m, compared with a pulse travelling the same distance through free space. A pulse at 5 GHz would be delayed by four times this amount. We will consider these delays again when we discuss radar altimeters in chapter 8 and the Global Positioning System (GPS) in appendix 1.

The electron density in the ionosphere is very variable, both temporally and spatially. The ionisation is significantly greater on the Earth's sunlit side than on the night side, it is strongly affected by variations in solar activity, and its spatial distribution is correlated with both altitude and geomagnetic latitude. Figure 4.8 illustrates typical mid-latitude electron densities as functions of altitude for day and night. As we have seen in deriving equation (4.23), the the integrated electron density $\int Ndz$ through the whole of the ionosphere is an

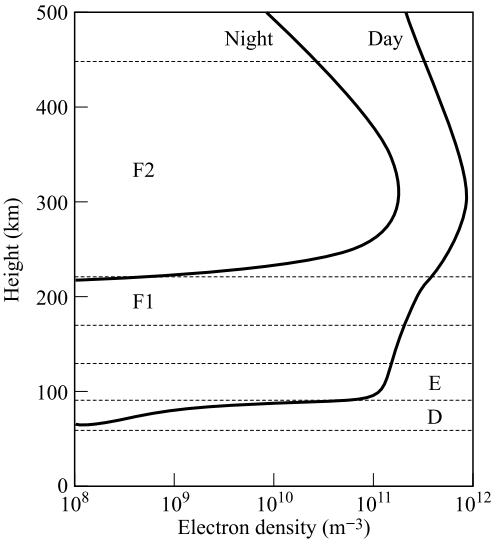

Figure 4.8. Typical electron densities in the ionosphere. The figure also shows the approximate positions of the layers into which the ionosphere is conventionally divided.

important quantity in considering the propagation time of microwave pulses. This quantity is often called the *total electron content* (TEC). It has a typical daytime value of $3 \times 10^{17}\,\mathrm{m}^{-2}$, and is usually about ten times less at night.

We remarked earlier that at frequencies below the plasma frequency, the dielectric constant of the ionosphere is negative. This implies that the refractive index is purely imaginary, and hence that radiation will be absorbed. The ionosphere is thus increasingly opaque as the frequency decreases below about 10 MHz, and this places a lower frequency limit on spaceborne remote sensing. (It does not apply to airborne techniques, of course, since these do not involve looking through the ionosphere.) However, we can note in passing that the opacity of the ionosphere at sufficiently low radio frequencies does have a beneficial effect, since it allows HF ('short wave') radio signals to propagate for long distances round the Earth's surface by bouncing between the surface and the ionosphere.

4.6 Atmospheric turbulence

One further and potentially important influence that the atmosphere can have on the propagation of electromagnetic radiation is as a result of atmospheric turbulence. This is always present to a greater or lesser extent in the lower atmosphere, and causes variations in the density, and hence refractive index, of the air. The phase of an electromagnetic wave is corrupted by these variations, and this adversely affects the behaviour of an imaging system.

The most useful way to describe the effects of this kind of phase fluctuation, which is of course statistical rather than deterministic, is by specifying the

structure function. This is usually defined as the variance of the phase difference between two points which would, in the absence of such effects, be in phase. It is therefore measured in radians squared, and is usually a function of the wavelength of the radiation as well as of the separation between the two points. The time-scale over which the phase variance is measured is also often important.

So far as the effect on the resolution of an imaging system is concerned, an approximate idea can be obtained by replacing the turbulent medium by a notional aperture whose size is equal to the separation at which the structure function reaches a value of 1 radian squared. For visible light travelling through the whole of the Earth's atmosphere, this separation is typically 0.2 m, corresponding to an angular resolution (calculated from the diffraction formula, equation (2.42)) of about 3×10^{-6} radians or about 1 second of arc. This scattering angle, which we will denote by $\Delta\theta$, is the limiting angular resolution that can be achieved by an *upward*-looking observation (such as an astronomical observation) through the whole atmosphere. However, for a *downward*-looking observation we also need to consider the effective height at which the scattering occurs. We will take this to be the scale-height of the atmosphere (of the order of 8 km), which we will denote by H, and we will assume that the observation is made from a height much greater than H. In our very simplified model, we will assume that all the scattering takes place at the height H.

Figure 4.9a shows a ray AS propagating obliquely through the atmosphere at an angle $\Delta\theta$ to the vertical. At S, it is scattered into a cone of directions from SE, which is clearly vertical, to SD. Figure 4.9b similarly shows the scattering of the ray BS, where S is the same point as in figure 4.9a. We can see, therefore, that a downward-looking observation from directly above the point S will collect radiation originating from any point between A and B. The distance between these points is approximately $2H\,\Delta\theta$, so this is the limiting *linear* resolution that is achievable. Substituting the values for H and $\Delta\theta$, we find that this limiting resolution is of the order of 5 cm.

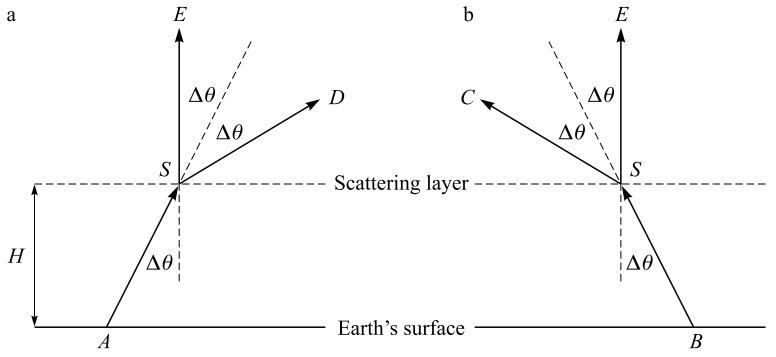

Figure 4.9. Schematic representation of the scattering of light travelling through the atmosphere. (a) The ray AS is scattered into the cone of directions between SE and SD; (b) the ray BS is scattered into the cone of directions between SC and SE.

Turbulence in the lower atmosphere causes similar effects at radio frequencies. However, for observations from satellites at radio frequencies, the *ionosphere* poses a potentially more serious problem. It is not really possible to quote a typical value for the ionospheric structure function because of the great variability alluded to earlier, but we may note that the phase variance will be proportional to λ^2 (because of the plasma dispersion relation, discussed in section 4.5), and that it will be greater near the geomagnetic poles and equator, and during the daytime.

PROBLEMS

1. Show that Doppler broadening will dominate over pressure broadening of a spectral line for a gas at temperature T and pressure p provided that the wavelength of the spectral line is less than $kT/p\sigma$, where σ is the collision cross-section defined in equation (4.11).

2. The attenuation coefficient of a typical tropospheric aerosol is $0.1\,\mathrm{km}^{-1}$ at sea level, and the total optical thickness of the aerosol for a vertical path through the atmosphere is 0.2. By assuming that the density, and hence the attenuation coefficient, of the aerosol obeys a negative exponential distribution with height (i.e. similar to equation (4.4)), calculate the scale height of the aerosol layer.

3. The meteorological visibility in fog is defined as the distance that gives an optical thickness of 4. If a typical fog has a mass density of 10^{-3} kg water per cubic metre and gives a visibility of 100 m, estimate the size of the water droplets.

4. Use equation (4.16) to show that, at low microwave frequencies, the absorption coefficient of a cloud of water droplets is given approximately by

$$0.5\left(\frac{\rho}{\mathrm{kg\,m^{-3}}}\right)\left(\frac{f}{\mathrm{GHz}}\right)^2 \mathrm{dB\ km^{-1}}$$

(i.e. independent of the droplet size), where ρ is the mass of water in kilograms per cubic metre of cloud. Assume that, for water at microwave frequencies, $\varepsilon_p = 75.9$, $\varepsilon_\infty = 4.5$ and $\tau = 9.2$ ps. Hence, by assuming that this relationship holds throughout the microwave region, discuss the statement that clouds are transparent to microwave radiation. Consider only absorption; that is, ignore any scattering from the droplets. Cloud water content ranges typically from $10^{-6}\,\mathrm{kg\ m^{-3}}$ for haze to $10^{-2}\,\mathrm{kg\,m^{-3}}$ for cumulonimbus.

5. Use the data of table 4.3 to estimate the effective raindrop radius, number density and sedimentation rate for rain rates of 1 and 100 mm h^{-1}, assuming that all the drops are spherical and have the same radius.